

# The easy magnetization directions in $R_6Fe_{23}$ intermetallic compounds: A crystal field analysis

G. J. Bowden, J. M. Cadogan, and H. de Leon  
*School of Physics, The University of New South Wales, Sydney, NSW 2052, Australia*

D. H. Ryan  
*Physics Department, McGill University, 3600 University St., Montreal, Quebec, H3A 2T8, Canada*

X-ray diffraction patterns on magnetically aligned powder samples of  $R_6Fe_{23}$  ( $R=Dy, Er, Ho,$  and  $Tm$ ) show that these compounds all magnetize along a  $[111]$  easy direction. At first sight it is difficult to reconcile the common easy magnetization direction of  $Er_6Fe_{23}$  and  $Tm_6Fe_{23}$  on one hand, with  $Dy_6Fe_{23}$  and  $Ho_6Fe_{23}$  on the other, since the respective  $B_{20}$  rare earth crystal field parameters of these pairs of compounds are opposite in sign. In this article we show that the crystal field stabilization energy of the  $[111]$  direction, relative to either  $[100]$  or  $[110]$ , varies as the square of the crystal field term  $B_{20}$ , thereby providing an explanation for the common  $[111]$  direction of easy magnetization. © 1997 American Institute of Physics. [S0021-8979(97)19908-X]

## I. INTRODUCTION

Previous studies of the cubic compounds  $R_6Fe_{23}$  ( $R$  = heavy rare earth) have shown that the preferred direction of magnetization is  $[100]$  for  $Y_6Fe_{23}$ <sup>1</sup> and  $[111]$  for  $R_6Fe_{23}$  ( $R=Dy,$ <sup>2</sup>  $Ho,$ <sup>3</sup> and  $Er$ <sup>4</sup>). Many of these directions were deduced from Mössbauer experiments and are somewhat tentative, because of the presence of many overlapping Fe sub-spectra.

The  $R_6Fe_{23}$  compounds are isomorphous with the  $Th_6Mn_{23}$  structure and belong to the cubic space group  $Fm\bar{3}m$  (No. 225). The  $R^{3+}$  ions occupy the  $24e$  sites, in four groups of six ions, with the *tetragonal* point symmetry  $4mm$ , while the Fe atoms are shared between the  $4b$  ( $m\bar{3}m$ ),  $24d$  ( $mmm$ ),  $32f_1$  ( $3m$ ), and  $32f_2$  ( $3m$ ) sites.<sup>5,6</sup> Gubbens<sup>4</sup> reported both x-ray and Mössbauer experiments on  $Er_6Fe_{23}$  and  $Y_6Fe_{23}$  and on the basis of the x-ray patterns of magnetically aligned samples he concluded that  $Er_6Fe_{23}$  magnetizes along the  $[111]$  direction at room temperature whereas  $Y_6Fe_{23}$  magnetizes along  $[001]$ . Nevertheless, we note that Gubbens' x-ray data for  $Er_6Fe_{23}$  show an enhancement of the (440) peak, contrary to the work reported here.

In this article we report the results of x-ray powder diffraction experiments on magnetically aligned  $Dy_6Fe_{23}$ ,  $Er_6Fe_{23}$ , and  $Tm_6Fe_{23}$  samples. These compounds were chosen because of the differing signs of their  $\alpha$ ,  $\beta$ , and  $\gamma$  Stevens coefficients. Rather surprisingly, we find that the three compounds share a common  $[111]$  direction of easy magnetization and we shall show that this result can be understood in terms of the strong quadratic  $B_{20}O_{20}$  crystal field interactions at the  $R^{3+}$  sites.

## II. EXPERIMENTAL DETAILS AND RESULTS

The samples were prepared in an argon arc furnace, annealed at  $1150^\circ C$  for six days and subsequently rapidly quenched to room temperature. They were examined by x-ray powder diffraction (XRD) on a Siemens D-5000 diffractometer using  $CuK\alpha$  radiation. The Curie temperatures were determined by thermogravimetric analysis using a Perkin-Elmer TGA-7 analyzer. The samples were virtually

single phase with Curie temperatures at  $261(2)^\circ C$  for  $Dy_6Fe_{23}$ ,  $230(2)^\circ C$  for  $Er_6Fe_{23}$ , and  $226(2)^\circ C$  for  $Tm_6Fe_{23}$ .

The XRD samples were prepared by grinding the materials under acetone. Magnetically aligned samples were produced by mixing the powder with a small amount of araldite and allowing the mixture to set in a magnetic field of 2 T. The cubic lattice parameters determined by XRD are  $12.05(5) \text{ \AA}$  for  $Dy_6Fe_{23}$ ,  $11.99(3) \text{ \AA}$  for  $Er_6Fe_{23}$ , and  $11.97(5) \text{ \AA}$  for  $Tm_6Fe_{23}$ . The powder diffraction patterns of the magnetically aligned samples show a strong suppression of the (400) and (440) peaks with strong enhancement of the (222) and (333) peaks. We conclude therefore that each of these compounds magnetizes along the  $[111]$  crystallographic axis of the  $Fm\bar{3}m$  cubic crystal structure, at least at room temperature.

Alternating current susceptibility measurements were made on a Lake-Shore closed-cycle susceptometer (400 A/m and 137 Hz) over the temperature range of 12–300 K.

## III. CRYSTAL FIELD CALCULATIONS

We can use the point charge model<sup>7</sup> to estimate the crystal field parameters at the rare earth site in  $R_6Fe_{23}$ . This reveals that with respect to their tetragonal local axes, the  $R^{3+}$  crystal field Hamiltonian is given by:

$$H_{cf} = B_{20}O_{20} + B_{40}O_{40} + B_{44}^cO_{44}^c + B_{60}O_{60} + B_{64}^cO_{64}^c. \quad (1)$$

The relationship between the crystal axes, and those associated with the point symmetry of the six  $R^{3+}$  ions is summarized in Fig. 1. It will be observed that only two of the R atoms, labeled  $B$ , possess local  $z$ -axes which coincide with the principal  $Z$ -axis of the crystal.

To estimate the relative strengths and signs of the crystal field parameters, point charge summations were made over a  $120 \text{ \AA}$  sphere. The results are summarized in Tables I and II. In preparing Table II, the magnitudes of the charges ascribed to the rare earth and iron atoms were set equal to  $+|e|$  and  $(1/6)|e|$ , respectively, based on consideration of the crystal field parameters determined for numerous intermetallics.<sup>8</sup> It will be seen that the quadratic crystal field coefficient  $B_{20}$  is dominant.

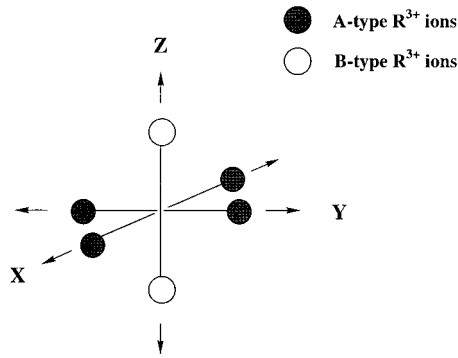


FIG. 1. Local axes of the six grouped  $R^{3+}$  ions in  $R_6Fe_{23}$ . The arrows indicate the local  $z$ -axis for each  $R^{3+}$  ion and  $\{X, Y, Z\}$  give the overall crystallographic principal axes.

#### IV. DIRECTION OF EASY MAGNETIZATION

For simplicity, we shall assume that with respect to its local axis the effective Hamiltonian for a given rare earth ion takes the form:

$$H = -g_j \mu_B \mathbf{J} \cdot \mathbf{B}_{\text{ex}} + B_{20} O_{20}, \quad (2)$$

where  $\mathbf{B}_{\text{ex}}$  is the effective exchange field at the rare earth site, generated primarily by the iron sublattice. Using molecular field theory,<sup>9</sup> we estimate  $\mathbf{B}_{\text{ex}}$  to be  $\sim 96$  T in  $Dy_6Fe_{23}$  at  $T=0$  K, based on Curie temperatures of 261 °C for  $Dy_6Fe_{23}$  and 208 °C for  $Y_6Fe_{23}$  (representing the Fe–Fe exchange).<sup>3,4</sup>

Given that the common direction of magnetization for  $Dy_6Fe_{23}$ ,  $Er_6Fe_{23}$ , and  $Tm_6Fe_{23}$  is  $[111]$ , as shown by the XRD work, it is advantageous to transform the above Hamiltonian to a new set of axes in which the new  $z$ -axis is collinear with the  $[111]$  direction.<sup>7</sup> With respect to these axes the Hamiltonian of Eq. (2) is transformed to:

$$H = -g_j \mu_B \mathbf{J} \cdot \mathbf{B}_{\text{ex}} + B_{20} \{-2\sqrt{2}O_{21}^c + O_{22}^c\}. \quad (3)$$

Note that (i) the diagonal crystal field term has been nullified, regardless of sign, and (ii) the transformation of Eq. (3) applies to all six  $R^{3+}$  ions shown in Fig. 1. Thus, the quadratic crystal field terms will not contribute to the energy of rare earth ion to leading order in  $B_{20}$ . However, the off-diagonal crystal field terms  $O_{21}^c$  and  $O_{22}^c$  will contribute to the energy of the ion in second order and we may use second order perturbation theory to deduce the crystal field contribution to the ground state energy of the  $R^{3+}$  ions. The contribution is

TABLE I. Point charge crystal field lattice summations  $\{A_{nm}\}$  in units of  $Ka_0^{-n}$  for the  $R^{3+}$  ion in  $R_6Fe_{23}$  ( $a_0$  is the Bohr radius). The point charges are  $Q_R$  and  $Q_{Fe}$ . To obtain the crystal field parameters  $\{B_{nm}\}$ , multiply by the relevant Stevens coefficients ( $\alpha, \beta, \gamma$ ), the  $4f$  electronic radial averages  $\langle r_{4f}^n \rangle$ , and the shielding parameters  $(1 - \sigma_n)$ .

$A_{20} = -688Q_R + 2210Q_{Fe}$
$A_{40} = 5.4Q_R - 6.6Q_{Fe}$
$A_{44}^c = -18.5Q_R + 54.4Q_{Fe}$
$A_{60} = 0.0204Q_R + 0.1695Q_{Fe}$
$A_{64}^c = -0.725Q_R + 1.627Q_{Fe}$

TABLE II. Crystal field parameters and energy terms  $B_{nm}\langle O_{nm} \rangle$  (at  $T=0$  K and ignoring quenching). These calculations assume  $Q_R = +1|e|$ ,  $Q_{Fe} = -(1/6)|e|$  and  $\sigma_2 = 0.5$ . Values of  $\langle r_{4f}^n \rangle$  are taken from Ref. 11.

Crystal field parameter (K)	$Dy_6Fe_{23}$	$Er_6Fe_{23}$	$Tm_6Fe_{23}$
$B_{20}$	+2.62	-0.95	-3.63
$B_{20}\langle O_{20} \rangle$	+275	-100	-240
$B_{40}$	$-5.8 \times 10^{-4}$	$+3.7 \times 10^{-4}$	$+1.2 \times 10^{-3}$
$B_{40}\langle O_{40} \rangle$	-9.5	+6.1	+7.1
$B_{60}$	$-4.9 \times 10^{-8}$	$-7.8 \times 10^{-8}$	$+1.9 \times 10^{-7}$
$B_{60}\langle O_{60} \rangle$	-0.044	-0.070	+0.032

$$\Delta E_g = \sum_{k \neq g} \frac{|\langle g | H_{cf} | k \rangle|^2}{E_g^0 - E_k^0}. \quad (4)$$

Taking  $Dy_6Fe_{23}$  as the test case for our crystal field calculations at  $T=0$  K and defining  $\Delta = (B_{20})^2 / g_j \mu_B B_{\text{ex}}$  we find that the ground state energy per  $Dy^{3+}$  ion is given by:

$$E_g = -g_j \mu_B (15/2) B_{\text{ex}} - 1522\Delta \quad (5)$$

to second order in  $B_{20}$ , which follows from the definitions of the operators  $O_{21}^c$  and  $O_{22}^c$ .<sup>7</sup> Note that the action of the off-diagonal terms is to reduce the energy of the ground state regardless of the sign of  $B_{20}$ .

For a  $[001]$  direction of magnetization, the crystal field interactions for the  $A$  and  $B$  rare earth atoms differ. For the two  $B$  atoms:

$$H = -g_j \mu_B \mathbf{J} \cdot \mathbf{B}_{\text{ex}} + B_{20} O_{20}, \quad (6)$$

whereas for the four  $A$  atoms:

$$H = -g_j \mu_B \mathbf{J} \cdot \mathbf{B}_{\text{ex}} - \frac{1}{2} B_{20} \{O_{20} \pm 3O_{22}^c\}. \quad (7)$$

For the overall group of six rare earth ions therefore, the energy of the ground state is unaffected by the crystal field to first order in  $B_{20}$ , as required by the cubic space group. However, the off-diagonal term in Eq. (7) will reduce the energy of the four  $A$  atoms. Once again, second order perturbation theory gives:

$$E_g = -g_j \mu_B (15/2) B_{\text{ex}} - 79\Delta \quad (8)$$

per  $Dy^{3+}$  ion.

For a  $[110]$  direction of magnetization, the respective  $R^{3+}$  Hamiltonians are

$$H_A = -g_j \mu_B \mathbf{J} \cdot \mathbf{B}_{\text{ex}} + B_{20} \{-\frac{1}{2}O_{20} + \frac{3}{2}O_{22}^c\} \quad (9)$$

and

$$H_B = -g_j \mu_B \mathbf{J} \cdot \mathbf{B}_{\text{ex}} + B_{20} \{\frac{1}{4}O_{20} \pm 3O_{21}^c - \frac{3}{4}O_{22}^c\} \quad (10)$$

and the energy for the  $[110]$  direction is:

$$E_g = -g_j \mu_B (15/2) B_{\text{ex}} - 1162\Delta. \quad (11)$$

From an examination of Eqs. (5), (8), and (11), it is clear that  $[111]$  is the favored direction of magnetization, irrespective of  $sign(B_{20})$ . We suggest, therefore, that (i) the quadratic crystal field at the rare earth sites in the  $R_6Fe_{23}$  intermetallic compounds is responsible for the common easy direction of magnetization, and (ii) the majority of the  $R_6Fe_{23}$  compounds will magnetize along the  $[111]$  direction,

regardless of the sign of their Stevens  $\alpha$  coefficient. The exceptions to this rule are, of course,  $\text{Y}_6\text{Fe}_{23}$  and  $\text{Gd}_6\text{Fe}_{23}$ , the former  $\text{R}^{3+}$  ion being nonmagnetic and the latter being  $S$ -state.

## V. DISCUSSION

It should be acknowledged that the above crystal field calculations have been performed for  $T=0$  K, whereas the measurements on the magnetically aligned samples were made at room temperature. Strictly speaking, therefore, it would be necessary to look for the minimum in the free energy  $F$  rather than the minimum in the ground state energy. However, we have also carried out ac-susceptibility measurements on each sample down to 12 K to check for possible spin-reorientations below room temperature; none was found. At low temperatures, the magnetocrystalline anisotropy associated with the second, fourth, and sixth order crystal field terms will fall according to  $[M(T)/M(T=0 \text{ K})]^{n(n+1)/2}$ , where  $M(T)$  is the magnetization of the  $R$  sublattice, and  $n=2, 4$ , and  $6$ , respectively.<sup>10</sup> Thus, at room temperature the fourth and sixth order anisotropy terms can be safely neglected<sup>11</sup> and magnetic alignment of the  $R$

sublattice will be determined primarily by the second order crystal field terms.

## ACKNOWLEDGMENTS

G. J. B. and J. M. C. are grateful to the Australian Research Council for its support. D. H. R. acknowledges support from the Natural Sciences and Engineering Research Council of Canada and the Fonds pour la formation de chercheurs et l'aide à la recherche (Québec).

<sup>1</sup>P. C. M. Gubbens, J. H. F. van Apeldoorn, A. M. van der Kraan, and K. H. J. Buschow, *J. Phys. F* **4**, 921 (1974).

<sup>2</sup>J. J. Bara, A. T. Pedziwiatr, and W. Zarek, *J. Magn. Magn. Mater.* **27**, 168 (1982).

<sup>3</sup>P. C. M. Gubbens (unpublished).

<sup>4</sup>P. C. M. Gubbens, Ph.D. thesis, Technische Hogeschool Delft, 1977 (unpublished), available from Delft University Press.

<sup>5</sup>A. S. van der Goot and K. H. J. Buschow, *J. Less-Common Met.* **1**, 151 (1970).

<sup>6</sup>M. P. Dariel and G. Erez, *J. Less-Common Met.* **22**, 360 (1970).

<sup>7</sup>M. T. Hutchings, *Solid State Phys.* **16**, 227 (1964).

<sup>8</sup>H. H. A. Smit, R. C. Thiel, and K. H. J. Buschow, *J. Phys. F* **18**, 295 (1988).

<sup>9</sup>J. F. Herbst and J. J. Croat, *J. Appl. Phys.* **55**, 3023 (1984).

<sup>10</sup>H. B. Callen and E. Callen, *J. Phys. Chem. Solids* **27**, 1271 (1996).

<sup>11</sup>A. J. Freeman and J. P. Desclaux, *J. Magn. Magn. Mater.* **12**, 11 (1979).